



RESEARCH ARTICLE

Generation and modulation of multiple 2D bulk photovoltaic effects in space-time reversal asymmetric 2H-FeCl₂

Liang Liu^{1,2}, Xiaolin Li¹, Luping Du³, Xi Zhang^{1,4,†}

¹ Institute of Nanosurface Science and Engineering, Guangdong Provincial Key Laboratory of Micro/Nano Optomechatronics Engineering, Shenzhen University, Shenzhen 518060, China

² School of Physics, State Key Laboratory for Crystal Materials, Shandong University, Jinan 250100, China

³ Nanophotonics Research Centre, Institute of Microscale Optoelectronics, Shenzhen University, Shenzhen 518060, China

⁴ Research Center of Plasma Medical Technology, Shenzhen University, Shenzhen 518060, China

Corresponding author. E-mail: †zh0005xi@szu.edu.cn

Received April 10, 2023; accepted June 6, 2023

Supporting Information

● The thickness effects on BPVEs

The thickness effects in the BPVEs of 2H-FeCl₂ mainly include three aspects. First, the systems with even layers present PT-symmetry, leading to the vanishing of shift-like photocurrents, injection-like photo-spin-currents and injection-like photo-orbital-currents. Second, the peaks of all kinds of photocurrents shift to lower photon energies along with the increasing of thickness. Third, the magnitudes of photocurrents and photo-orbital-currents are reduced with the increasing of thickness, while the photo-spin-currents are enhanced.

To clarify the thickness dependence in more details, the bilayer model and bulk model (that is, the case of infinite thickness) are investigated.

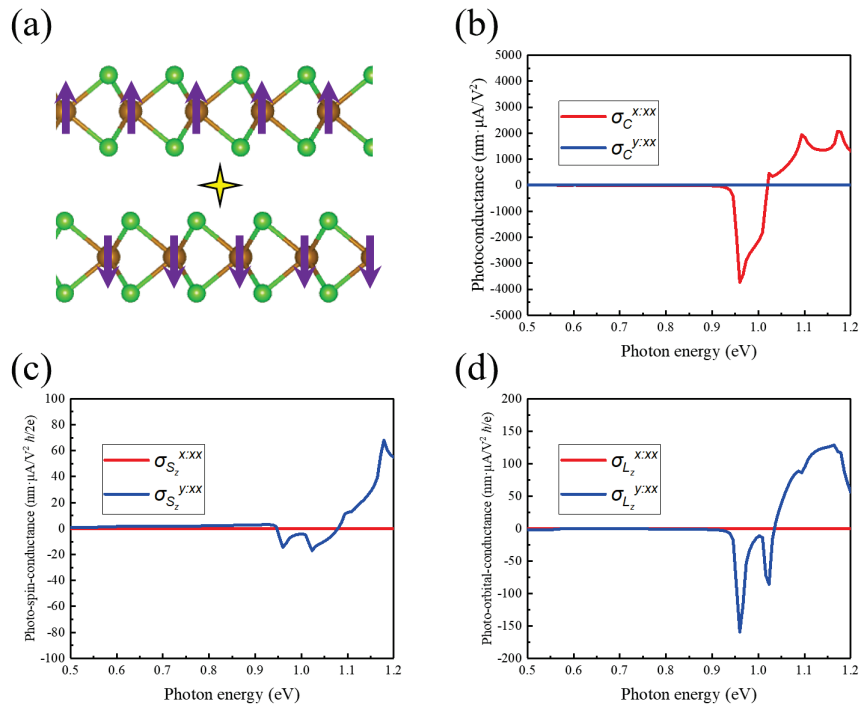


Fig. S1 The geometric, magnetic and BPVE structures of bilayer 2H-FeCl₂. **(a)** The geometric and magnetic structure of 2H-FeCl₂. The green and brown balls denote Cl and Fe atoms. The arrows represent the local magnetic moments on Fe atoms. The yellow star gives one of the possible inversion centers of PT-symmetries. **(b)** The 2nd order photoconductance of bilayer 2H-FeCl₂. **(c)** The 2nd order photo-spin-conductance. **(d)** The 2nd order photo-orbital-conductance.

The DFT calculations suggest that the bilayer 2H-FeCl₂ favors an A-type antiferromagnetic ground state with AB-stack, as shown in Fig. S1(a). Apparently, with the combined symmetry operations of time reversion and spatial inversion about the center marked in Fig. S1(a), all the geometric and magnetic structures coincide with themselves. So, the bilayer 2H-FeCl₂ displays the PT-conserved symmetry, and it should host the BPVE of class 2 (see Table 1 in main text). To clearly display the averaged BPVE efficiency of bilayer 2H-FeCl₂ with the monolayer, we set the thickness of bilayer to 2 nm, that is, double the case of monolayer in the following calculations on the photoconductances.

Fig. S1b shows the spectra of $\sigma_C^{x:xx}$ and $\sigma_C^{y:xx}$ of bilayer 2H-FeCl₂ with Néel vector along the +z-direction. First, $\sigma_C^{y:xx}$ vanishes everywhere due to the PT-symmetry. Besides, the first peak of $\sigma_C^{x:xx}$ occurs at photon energy 0.96 eV, which is slightly lower than the monolayer case (1.05 eV). The magnitude of the largest $\sigma_C^{x:xx}$ is -3738 ($\text{nm} \cdot \mu\text{A}/\text{V}^2$), also smaller than the monolayer one ($4620 \text{ nm} \cdot \mu\text{A}/\text{V}^2$). Hence, the interlayer interactions of bilayer 2H-FeCl₂ can shift the BPVE peaks to lower energy and reduce the efficiency of photo-to-current conversions.

Fig. S1c and S1d show the photo-spin-conductance and photo-orbital-conductance. The injection-like contributions $\sigma_{S_z}^{x:xx}$ and $\sigma_{L_z}^{x:xx}$ (red lines) vanish due to the PT-symmetry. For the shift-like parts, the largest photo-spin-conductance $\sigma_{S_z}^{y:xx}$ is 68 ($\text{nm} \cdot \mu\text{A}/\text{V}^2 \hbar/2e$), which is larger than the monolayer case ($-21 \text{ nm} \cdot \mu\text{A}/\text{V}^2 \hbar/2e$). And the largest photo-orbital-conductance $\sigma_{L_z}^{y:xx}$ is -159 ($\text{nm} \cdot \mu\text{A}/\text{V}^2 \hbar/2e$), smaller than the monolayer ($-183 \text{ nm} \cdot \mu\text{A}/\text{V}^2 \hbar/2e$).

To further reveal the BPVEs in the thick limit of 2H-FeCl₂, a bulk model is established as shown in Fig. S2a. The bulk 2H-FeCl₂ favors interlayer anti-ferromagnetic order and AB-stack, which is similar to the bilayer case. Hence, the bulk phase also presents the PT symmetry and belong to the class 2 BPVE. According to the DFT calculations, the thickness (the length of c-axis) of one cell of bulk 2H-FeCl₂ is ~ 1.20 nm. To compare the BPVE efficiencies more straightforwardly, the thickness of one cell is set to 2 nm in the following calculations on the BPVEs.

In line with the PT symmetry, bulk 2H-FeCl₂ only presents injection-like photocurrents, shift-like photo-spin-currents and shift-like photo-orbital-currents. Fig. S2b shows that the first peak of $\sigma_C^{x:xx}$ is -2516 ($\text{nm} \cdot \mu\text{A}/\text{V}^2 \hbar/2e$) at photon energy 0.93 eV. The position of peak is further lowered and the magnitude is also reduced than the bilayer case discussed above. Fig. S2c shows that the largest photo-spin-conductance $\sigma_{S_z}^{y:xx}$ is 81 ($\text{nm} \cdot \mu\text{A}/\text{V}^2 \hbar/2e$), larger than the bilayer case ($68 \text{ nm} \cdot \mu\text{A}/\text{V}^2 \hbar/2e$). Fig. S2d shows that the largest photo-orbital-conductance $\sigma_{L_z}^{y:xx}$ is -158 ($\text{nm} \cdot \mu\text{A}/\text{V}^2 \hbar/2e$), which is nearly the same as the bilayer ($-159 \text{ nm} \cdot \mu\text{A}/\text{V}^2 \hbar/2e$).

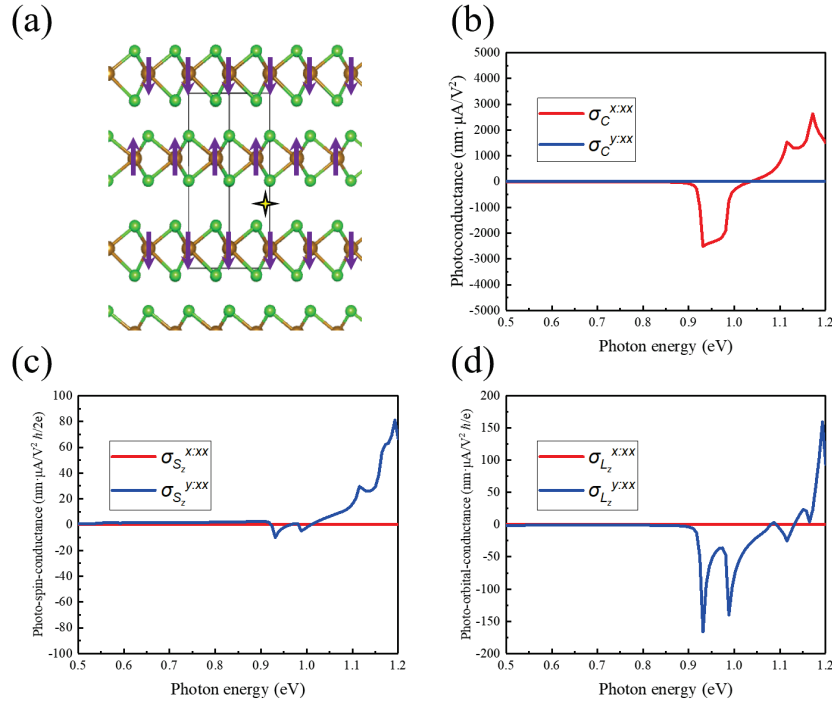


Fig. S2 The geometric, magnetic and BPVE structures of bulk 2H-FeCl₂. (a) The geometric and magnetic structure of 2H-FeCl₂. (b) The 2nd order photoconductance of bulk 2H-FeCl₂. (c) The 2nd order photo-spin-conductance. (d) the 2nd order photo-orbital-conductance.

Hence, the emergent PT-symmetry induced by the anti-ferromagnetism in bilayer and bulk phases of 2H-FeCl₂ annihilate the shift-like photocurrents, injection-like photo-spin-currents and injection-like photo-orbital-currents. Besides, the interlayer interactions can further renormalize the electronic structure and lead to the reductions on the injection-like photocurrents and shift-like photo-orbital-currents, while the shift-like photo-spin-currents are enhanced.